Control Strategies for Arrays of Wave Energy Devices

J. Westphalen*, G. Bacelli*, P. Balitsky* and J. V. Ringwood*
*Centre for Ocean Energy Research
Dept. of Electronic Engineering
National University of Ireland, Maynooth, Ireland
E-mail: jan.westphalen@eeng.nuim,.ie

***Abstract*—In this paper, we investigate the differences between two control strategies for a two-device linear array of wave energy converters (WEC) for device spacings of 4 to 80 times the device diameter. The WECs operate in heave only and are controlled in real time. The control strategies, called the independent device and global array control, estimate the excitation forces and calculate the optimum vertical velocity trajectory and reactive power take off force to achieve the velocity for a given sea state. The independent device controller assumes that each device is in isolation and only computes the excitation forces based on the incident wave, whereas the global array controller does take the radiation and diffraction effects from the other devices into account. Whatever controller is used in the simulations, all hydrodynamic coupling effects are accounted for.**

For a cylindrically shaped single-body device with diameter of 5 m and a draught of 25 m we simulate the device motions for 5 regular wave cases and one irregular sea state representing a Bretschneider spectrum.

These first test sets illustrate the different control needs depending on the separating distance of the array members. A global control algorithm is advantageous for small separating distances, where radiation is larger.

***Index Terms*—array interaction, control strategies, power optimization, boundary element method, linear theory**

NOMENCLATURE

η	surface elevation
γ	angle between F_e and u in the phasor plane
ω	wave frequency
A	wave amplitude
E	Fourier coefficients of excitation force
F_e	excitation force
H	Fourier coefficients of hydrodynamic added mass and damping
H_0	wave height
J	cost function
K	exciting force coefficient
P	Fourier coefficients of PTO force
P_e	average absorbed power
P_r	average radiated power
r	radius of cylinder
R_r	real part of radiation impedance
T	wave angular period
u	vertical velocity
X	Fourier coefficients of vertical velocities

Subscripts

c	constraint
G	global array control
I	independent device control

Superscripts

A	Body A
B	Body B

I. INTRODUCTION

For a single WEC, it is well known that the device needs to be controlled in order to maximize energy production [1], [2]. The need for control arises because the amount of energy captured is maximized when the resonance frequency and resistance of the device is matched to the resonance frequency and amplitude of the incoming wave. As a consequence away from resonance the device performs much more poorly [1]. Yet, because of the variable nature of ocean waves, the input wave frequency constantly changes. By controlling the device, one can modify its oscillatory motion to match the sea conditions resulting in significantly more energy capture [2]. While optimal control can provide significant advantages in terms of power output, careful consideration must be taken of the oscillation amplitude required, as it can in many cases exceed the stroke length and power limit of the device in addition to the modelling assumptions [3], [4]. Several different control algorithms have been developed that seek approach the optimal condition under one or several constraints, among them [3], [5]–[7]. An important point to consider is that, in order to apply the optimal control algorithms in real time, a prediction of the incident force is required, as shown in [8]. For irregular waves this is impossible to model in the frequency domain, as mentioned in [3] and, as a consequence, a time-domain simulation is required to model real-time control, for example as in [7], [9].

Extending these approaches to an array is not a trivial matter because the motion of each device is influenced by the others. Since any control scheme will modify the motion of a single device, it will also modify its influence on the other devices. Although these effects can be very difficult to quantify, a simple measure of their cumulative effects on power absorption in an array is the q-factor, introduced in 1979 in [10]. The q-factor is the power generated by an array of N devices divided by the power that would be generated by N single device. If $q > 1$, then the overall array power

absorption is greater than then sum of the power absorbed by the constituent devices in isolation. Conversely, if q <1, then the array hydrodynamics have a deleterious effect on power absorption. Whilst the hydrodynamic interactions in an array have been extensively studied since the early 1980s, for example in [11], [12] and [13], all of these studies assumed optimal control and small body dimensions compared to the incident wave length in addition to using regular waves.

Recently, however, a number of investigators have looked into more realistic scenarios where the control is modelled by a variable damping coefficient for a given sea state [4], [14]–[16]. Child and Venugopal [14] found that increasing the damping on the device compared with the optimal value reduces the constructive effects of radiation by reducing the device motion near the resonance peak. Folley and Whittaker [15] found a significant reduction in power when a devices is tuned away from the optimal frequency, with the result that the sub-optimal scenarios modelled prevent the WECs in the array to take advantage of the constructive effects of radiation, thus significantly reducing the overall power absorbed [15]. Both Cruz *et al.* [16] and de Backer *et al.* [4] calculated q-factors below one, irrespective of the control scheme they used. The results of these four investigations point to the need for a more sophisticated control scheme, that is better able to take advantage of the constructive interference of radiation in order to maximize array power production. Moreover, a better understanding of the effects of constraints on power production in an array is needed.

In this paper, we present the first results toward an implementation of a general time-domain control algorithm that can be applied to an array of WECs. The overall aim is to implement a real-time strategy that optimises the power output of a single device, a single multi-body device or such devices arranged in an array or wave farm. We investigate the need of a global optimisation algorithm based on the radiation properties of WECs near each other and the difference with respect to control that operates on an individual device level.

Computations are performed for two single-body devices of cylindrical shape extracting energy from the waves in heave motion only. The devices are controlled by applying a power take off (PTO) force that adjusts the vertical velocity in order to achieve maximum power conversion for the approaching wave. Two control algorithms are tested: one operating on an individual device level, also called independent device controller, and a global array control. The individual device controller does not take the interactions from the other devices into account and optimises the motion based on the incident and diffracted waves only. The global controller takes the hydrodynamic coupling of both devices into account and acts accordingly. Results are presented for a WEC of 5 m diameter, 25 m draught, for 5 different regular wave cases and one irregular sea representing a Bretschneider spectrum. Section II briefly describes the hydrodynamic model and control strategies. Results are presented in section III.

II. Formulation of Hydrodynamic Model and Control Strategies

A. Hydrodynamic Model

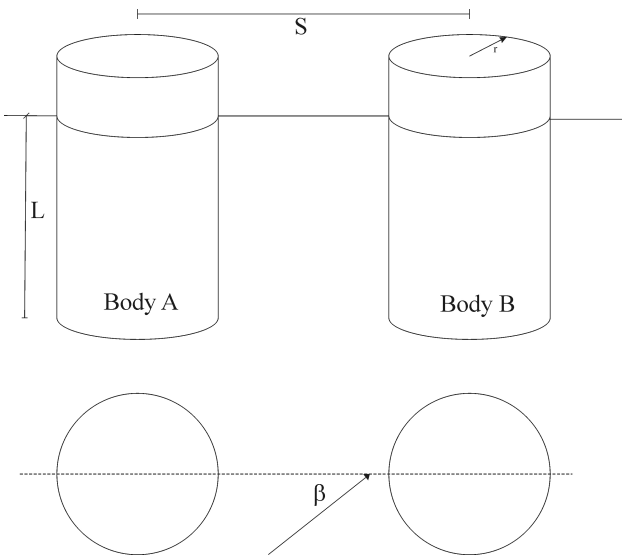

Fig. 1. Modelled geometry for body A and B, separation distance S, draught L, radius r and incident wave heading angle β

For this work we assume non-viscous, irrotational flow. The amplitude of the waves and device motions are small, which makes linear wave theory applicable and the hydrodynamic problem can be solved in the frequency domain. The interactions of the bodies due to the incident waves, the diffracted and radiated waves can then be described using potential theory. Here, the boundary element solver WAMIT ® [17] is used. This package is widely applied in studies of WEC arrays, as in [4], [15], [16]. Related cases are described, for example, in [18].

The geometry, that is modelled, can be seen in Figure 1. As the pressures and forces are only solved for the wetted surface, the density of the body ρ_b is set to 0.833 ρ_w (density of water) to give 5 m "dry" body height above the still water level. 5 m is also the maximum amplitude constraint used for the time domain simulations of the controller (see Section II-B). The draught is set to 25 m to achieve a resonant period of the body of approximately 10 s [19], which coincides with the peak period of the Bretschneider spectrum used for the simulation of the controlled WECs. In WAMIT ® the high order method is used and computations are performed for 300 frequencies equally spaced at intervals of 0.0341 rad/s.

B. Control Strategies

The control algorithm used in this paper is adapted from an isolated self reacting two-body wave energy converter. The strategy is described in detail in [9] and will only be outlined briefly here. For the results presented here, knowledge of the surface elevation time history is assumed. In reality, prediction is possible for a time window large enough for the controller to act on the device and tune it to the incoming wave [8], which

makes it possible to use control algorithms in real-time. Errors in the prediction of the wave elevation result in degradation of the controller performance. For this paper, however, the objective is to compare two different control strategies; since prediction errors affect both controllers in the same manner, the relative performance between the controllers is not affected by prediction errors, therefore they will not be considered. From the wave spectrum, the excitation forces F_e on each body are calculated based on

$$F_e(\omega) = K(\omega)\,\eta(\omega) \tag{1}$$

where K is the exciting-force coefficient computed by WAMIT ® and η is the wave elevation. The next step is to calculate the optimum vertical velocity trajectory for the wave experienced by the devices, solving the linear system

$$X = H(E - P), \tag{2}$$

which is obtained by discretising the time domain equation of motion of the buoys. The discretisation is carried out by approximating the motions and the forces acting on the bodies using a linear combination of basis functions [9], [20]. The work presented in this paper is based on the approximation by means of a truncated Fourier series: P is the vector of the Fourier coefficients of the PTO forces, E is the vector of the Fourier coefficients of the excitation forces and X is the vector of the Fourier coefficients of the velocities, all given as

$$P = \begin{bmatrix} P^A \\ P^B \end{bmatrix}, \tag{3}$$

$$E = \begin{bmatrix} E^A \\ E^B \end{bmatrix} \tag{4}$$

and

$$X = \begin{bmatrix} X^A \\ X^B \end{bmatrix}. \tag{5}$$

where superscripts A and B refer to body A and body B, respectively. The converted energy is described by a quadratic cost function $J(P)$ and the optimal PTO force is calculated by minimizing $J(P)$ with respect to P.

1) Global Array Control: In the global controller, all hydrodynamic effects are taken into account. Therefore the cost function is given as

$$J_G = P^T H(E - P) = -P^T H P + P^T H E \tag{6}$$

with

$$H = \begin{bmatrix} H_{11} & H_{12} \\ H_{21} & H_{22} \end{bmatrix} \tag{7}$$

and

$$P = \begin{bmatrix} P^A \\ P^B \end{bmatrix}. \tag{8}$$

The hydrodynamic coupling appears in the off-diagonal terms of the matrix H, i.e. H_{12} and H_{21}.

2) Independent Device Control: For the individual device controller the cost function J_I is

$$J_I = P^{A^T} X^A + P^{B^T} X^B,$$

which can be written in the same form of Equation 6 setting the cross-coupling terms H_{12} and H_{21} to zero, such as:

$$J_I = -P^T \begin{bmatrix} H_{11} & 0 \\ 0 & H_{22} \end{bmatrix} P + P^T \begin{bmatrix} H_{11} & 0 \\ 0 & H_{22} \end{bmatrix} E. \tag{9}$$

III. Simulation Results for Different Array Configurations

The software simulates the motion of the devices, the PTO forces, the instantaneous converted power and the vertical velocities and displacements of the WECs for a representative surface elevation time-history of a given wave spectrum. Amplitude constraints between 1 and 5 m are applied for simulations where the waves are 4 m high. No constraints are used for the small-wave simulations presented here.

In order to simplify the results and be able to separate out effects such as radiation and diffraction, regular waves are simulated. Table I shows the different settings for which results are presented in this section, where the wave heights H_0, the wave periods T and the wavelengths λ are given.

When there are multiple bodies, interaction between the bodies is caused by both radiation and diffraction. Diffraction only depends on the incoming waves for any fixed body geometry and array configuration, while radiation depends on the body motion, which is calculated by the controllers. If constraints are not considered, the control algorithm, as described in the previous section, provides the same velocity profile as reactive control, which is known to produce large oscillations, thus large radiated waves even for small incident waves.

The difference between the global and independent controller is that the global controller also takes into account the coupling due to radiation when computing the control signal. If the effect of radiation on one device due to the other one is small, then the difference between the control signals computed by both strategies is small. For controlled devices in an array the interaction is the largest when the constraints are not active. Hence, if the interaction is small for the unconstrained case, then it will be small also for the constrained. This fact can be seen, for the case of a monochromatic incident wave, considering the average radiated power P_r and the average absorbed power P_e, as defined in [19]:

$$P_e = \frac{1}{2}\mathrm{Re}\{F_e\, u^*\} = \frac{1}{2}|F_e||u|\cos(\gamma) \tag{10}$$

$$P_r = \frac{1}{2}R_r|u|^2 \tag{11}$$

where F_e and u are the excitation force and the vertical velocity of the buoy in the phasor domain, R_r is the real part of the radiation impedance and γ is the angle between the excitation force and the velocity in the phasor plane. If

the buoy is controlled with reactive control [19], the optimal velocity is

$$\hat{u} = \frac{F_e}{2\,R_r} \tag{12}$$

and $\gamma = 0$, thus the ratio between the average radiated power and the average absorbed power is $P_r/P_e = 0.5$. If constraints are active then the optimal oscillation velocity $\hat{u}_c$ is smaller or equal than the unconstrained case, that is

$$|\hat{u}_c| \leq |\hat{u}| = \frac{|F_e|}{2\,R_r} \tag{13}$$

and the ratio $P_r/P_e \leq 0.5$ (assuming $\gamma = 0$ to maximise absorption). Therefore, for any amplitude of the incident wave, when constraints are active the interaction between the two buoys due to radiation is smaller than the situation when constraints are not active.

All sea states are simulated for deep-water conditions and the device/array geometry described in Section II with a radius r of 2.5m, draught L of 25m and 31 relative separation distances $S/(2r)$ between 4 and 80.

TABLE I
PROPERTIES OF SIMULATED WAVE CLIMATES

	H_0 [m]	T [s]	λ [m]
Bretschneider	0.1, 4	10	156
Regular wave 1	0.1, 4	9.81	150
Regular wave 2	0.1, 4	6.94	75
Regular wave 3	0.1, 4	7.5	87
Regular wave 4	0.1, 4	8	100
Regular wave 5	0.1, 4	9	125

A. *Controller performance in regular waves*

The mean converted energy of the array is normalised with twice the mean converted power of a single isolated device operating in the same sea state. This gives the q-factor for each spacing as a measure of array performance.

For regular waves of 0.1 m height and periods between 6.94 and 9.81s the q-factors can be seen in Figures 2 - 6. In all 5 graphs high array efficiencies for *both control strategies* can be identified at spacings equal to multiples of half the incident wavelength. Then the devices are oscillating either in opposite phase or in phase as shown in Figures 7 and 8 for β = 0 deg, T = 9.8s and relative spacings $S/(2r)$ = 15 and 30. When the array performs badly, less motion of the downstream device can be observed resulting in less energy being converted (Figure 9, β = 0 deg, T = 9.81s, $S/(2r)$ = 22).

The magnitude of the q-factors varies from 0.5 to 0.94. This means that even when the devices are in phase, less energy is converted than for the same number of isolated devices. Furthermore, the q-factor seems to converge towards a value of 0.6 with increasing distance. This is probably due to a shielding effect for heading angle β = 0 degree.

Between the two control strategies, only small differences can be identified. Generally, the global array controller performs slightly better. However, for small separating distances one would expect larger influence of the global controller on the overall power production of the array, as it takes the interaction effects into account within the computation of the cost function (Equations (6) and (9)), i.e. the cross coupling terms H_{12} and H_{21}.

For 90 degree heading angle the shielding effect should be eliminated and diffraction effects should be minimised for the given sea state of 10 cm height. Thus, the controllers mainly take the motion of the other devices into account when computing the optimal velocity profile for which maximum energy conversion occurs. Figure 10 shows the q-factors for such a situation (β = 90 degree, T = 9 s). The differences in the performance of the global and independent controller are relatively large for small separating distances and vanish further away. The overall performance for this heading angle converges to q = 1. This means that shielding effects are minimised, as one would expect for devices that are arranged side by side. However, peak performances in this data set occur at distances equal to the incident wave length. This must be due to constructive interference caused by diffraction.

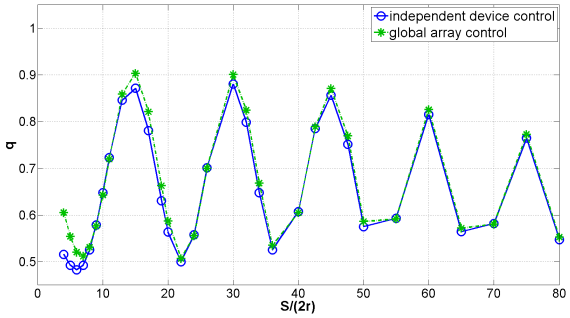

Fig. 2. q-factor for device spacings $S/(2r)$ in regular wave, β = 0 degree, T = 9.81 s, H_0 = 0.1 m

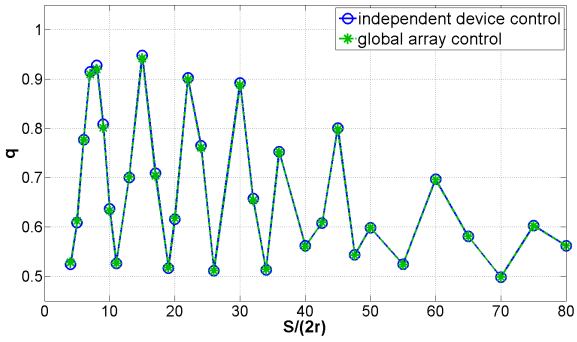

Fig. 3. q-factor for device spacings $S/(2r)$ in regular wave, β = 0 degree, T = 6.94 s, H_0 = 0.1 m

When the waves become larger, the amplitude constraints become active and restrict the vertical motion of the devices,

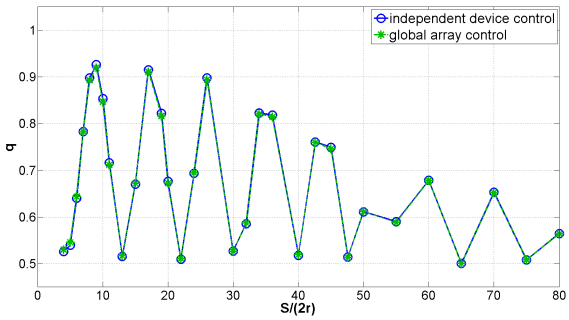

Fig. 4. q-factor for device spacings $S/(2r)$ in regular wave, β = 0 degree, T = 7.5 s, H_0 = 0.1 m

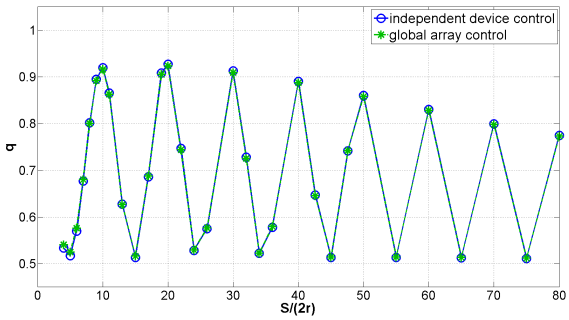

Fig. 5. q-factor for device spacings $S/(2r)$ in regular wave, β = 0 degree, T = 8.0 s, H_0 = 0.1 m

which was the case for all large-amplitude regular wave cases. Here, waves of 2 m amplitude were simulated and amplitude constraints of 1, 2, 3, 4 and 5 m were imposed on the devices, where both WECs had the same constraint for a given simulation. Figures 11 and 12 show the q-factors for all devices for heading angles β = 0 and 90 degree and active constraint of 3 m. Figures 13 and 14 show the corresponding displacements for $S/2r$ = 22, which show the motion of the devices within the bounds of +/- 3 m. The difference in the q - factors between the global and independent controller are zero for all constraints, when they are active. The absolute power generated by the device, of course, increases with the amplitude, that it is allowed to move.

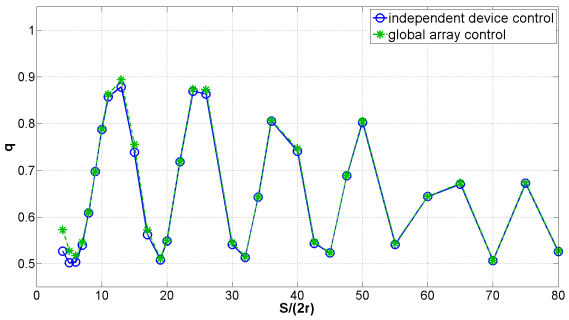

Fig. 6. q-factor for device spacings $S/(2r)$ in regular wave, β = 0 degree, T = 9.0 s, H_0 = 0.1 m

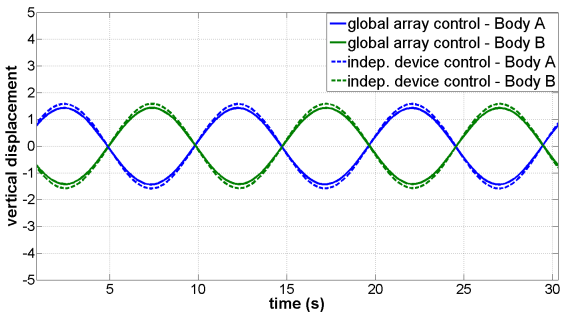

Fig. 7. Displacements for WECs for global and independent control at $S/(2r)$ = 15, T = 9.81s, β = 0 degree, H_0 = 0.1 m

B. *Controller performance for polychromatic seas*

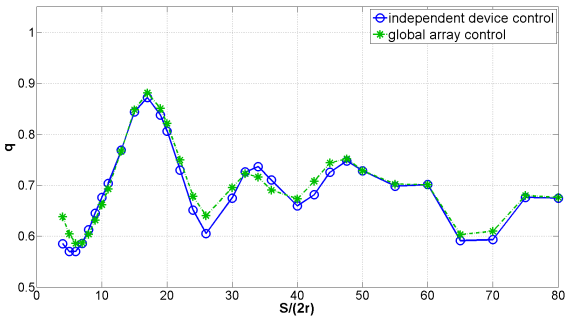

Fig. 15. q-factors for all device spacings for the Bretschneider spectrum (H_0 = 0.1 m) and heading angle β = 0 degree

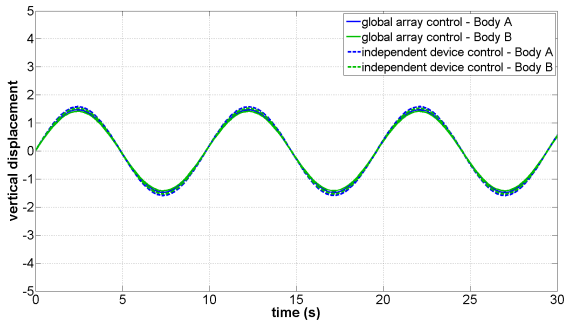

Fig. 8. Displacements for WECs for global and independent control at $S/(2r)$ = 30, T = 9.81s, β = 0 degree, H_0 = 0.1 m

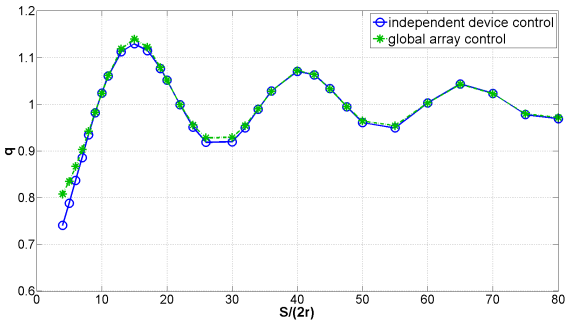

Fig. 10. q-factor for device spacings $S/(2r)$ in regular wave, β = 90 degree, T = 9.0 s, H_0 = 0.1 m

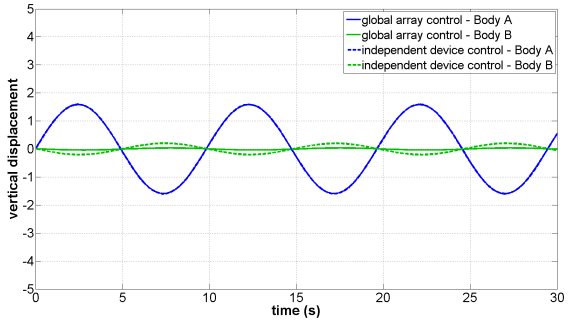

Fig. 9. Displacements for WECs for global and independent control at $S/(2r)$ = 22, T = 9.81s, β = 0 degree, H_0 = 0.1 m

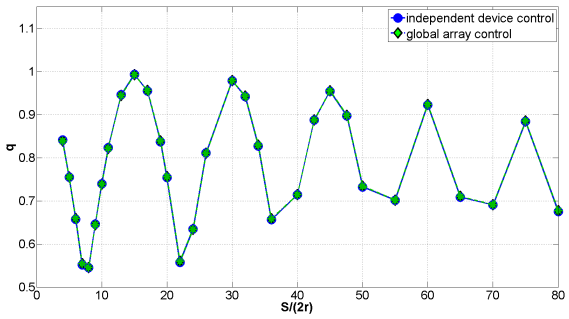

Fig. 11. q-factor for device spacings $S/(2r)$ in regular wave, β = 0 degree, T = 9.81 s, H_0 = 4 m

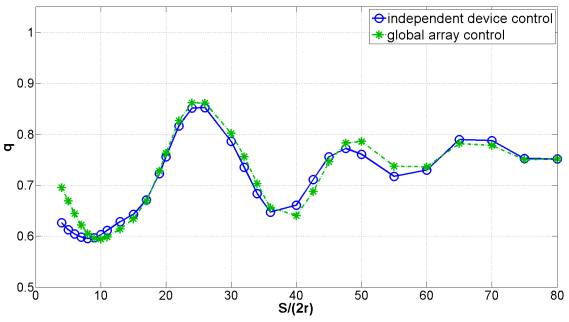

Fig. 16. q-factors for all device spacings for the Bretschneider spectrum (H_0 = 0.1 m) and heading angle β = 45 degree

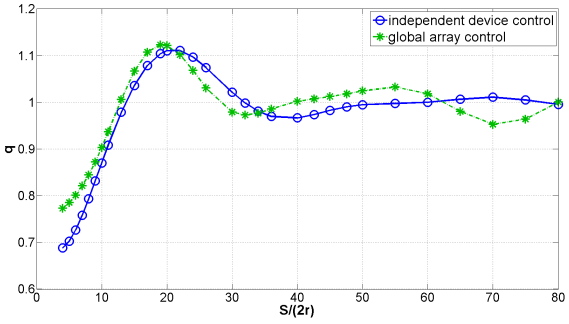

Fig. 17. q-factors for all device spacings for the Bretschneider spectrum (H_0 = 0.1 m) and heading angle β = 90 degree

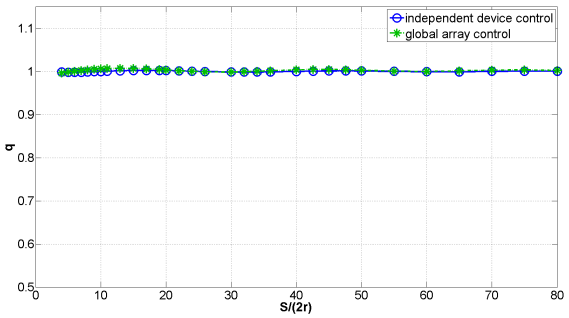

Fig. 12. q-factor for device spacings $S/(2r)$ in regular wave, β = 90 degree, T = 9.81 s, H_0 = 4 m

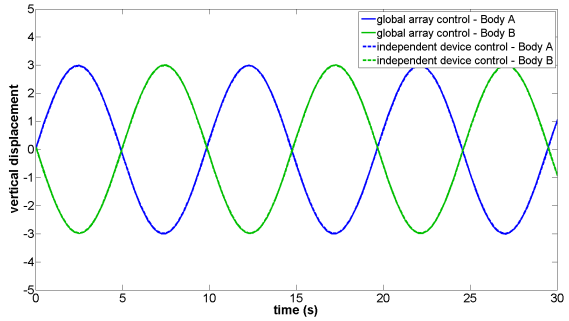

Fig. 13. Displacements for WECs for global and independent control at $S/(2r)$ = 22, T = 9.81s, β = 0 degree, H_0 = 4 m

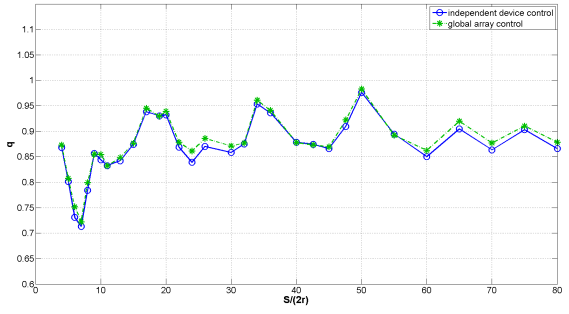

Fig. 18. q-factors for all device spacings for the Bretschneider spectrum (H_0 = 4 m) and heading angle β = 0 degree

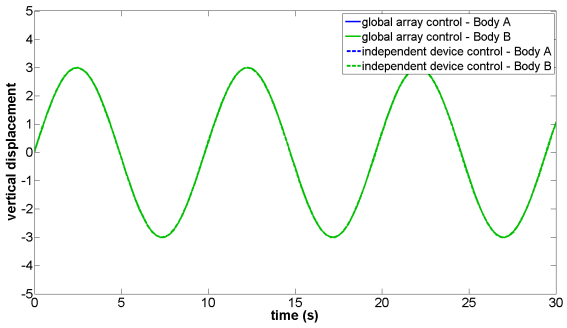

Fig. 14. Displacements for WECs for global and independent control at $S/(2r)$ = 22, T = 9.81s, β = 90 degree, H_0 = 4 m

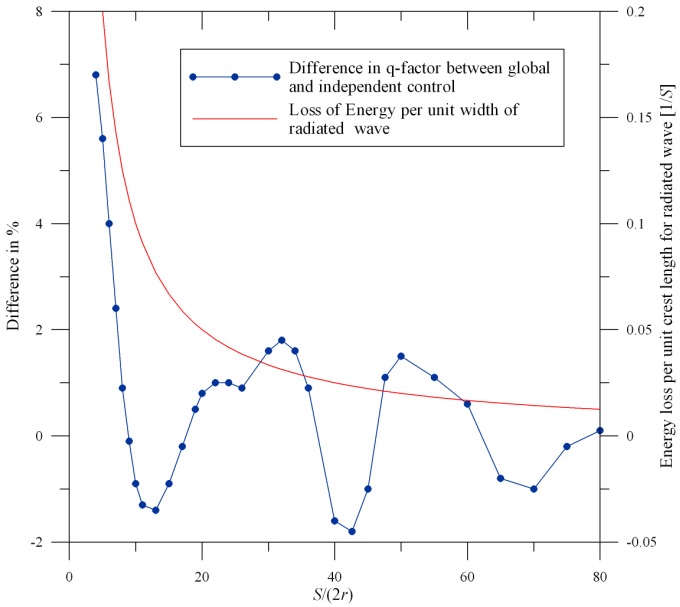

Fig. 19. Energy loss in radiated (circular) wave with distance from source and differences in q-factor for independent and global control for all spacings

For more realistic comparisons, an irregular sea state has also been simulated. All devices experience the same surface elevation and simulations are performed for 600 s. The q-factors are calculated as before, i.e. based on the mean absorbed power over the simulation time. For H_0 = 10 cm and T = 10 s the q-values are shown in Figures 15 - 17. As for the regular waves, the differences between the independent and global controller are small except for small device spacings. Overall the variation of q-factors with respect to the spacing of the devices is less pronounced than in regular waves, which is expected and due to the variation in frequencies and wave heights for the irregular sea. However, peak performances occur at spacings $S/(2r)$ = 0.55 λ and multiple integers of this value for β = 0 degree. When the waves approach the array at an angle of 45 degree the peak is shifted to 0.8 λ, as shown in Fig. 16.

For the large-amplitude Bretschneider sea, the differences in the q - factors between the global and independent controllers vanish, as it can be seen in Fig. 18 for β = 0 degree and

constraint of 3 m.

IV. Conclusions

Results are presented for two control strategies of WECs arranged in an array and operating in heave only. Here, we use a very simplistic approach of two devices and different spacing configurations. Simulations are done for 5 regular waves and also one irregular sea state representing a Bretschneider spectrum with peak frequency at the natural frequency of the device.

The simulations consist of two parts: the control algorithm estimates the optimum PTO force to achieve the optimum velocity and power capture for the approaching wave. The device is simulated with these settings for the sea state by solving the equations of motions in the time domain. From these the instantaneous converted power is used for the assessment of the performance of the device and array configuration for both control strategies. The actual velocity of the device is not calculated.

For the independent device controller the other device does not exist and only the excitation from the incident wave is included in the estimation. The cost function is optimised for each device individually. The time domain simulation however is done for the full interaction of both devices, which naturally results in a difference in prediction by the controller and experienced wave.

The global controller takes the hydrodynamic interactions between the two devices into account, including radiation effects. The cost function is solved to optimise the total power conversion of the array. In this way, each device is commanded not only to optimise its own favour, but also to provide an optimum radiated wave to the other device.

At this stage and for the presented data set the differences are small between an array, in which the devices are controlled individually or globally with regards to the total array power output. Differences could be identified for small sea states at close devices spacings, where hydrodynamic coupling from radiation occurs, which then becomes large relative to the incident wave. Hence, closely spaced arrays, such as the Manchester Bobber or Wavestar, could benefit from a global control algorithm. However, as differences between the two control strategies only occur when radiation effects are large compared to diffraction, an independent (individual) controller seems preferable than the global, as it does not require information about the state of the other devices.

The effect, that the difference in the controller performances vanish with the separating distance of the devices can be illustrated when the differences in q-factors are plotted against the distance. As the energy in a wave remains constant when it travels, but for a circular wave the circumference increases with distance from the source of radiation, the energy per unit-length wave crest decreases at a rate of $1/S$. In Figure 19, this function is plotted against the separating distance with the differences of the q-values of Figure 16. Both graphs coincide for small distances.

It seems very important to reduce destructive interference by optimising the array spacing based on wave climate and diffraction effects in the first place.

As these are early-stage results further tests are necessary and results for more devices with different dimensions, i.e. draughts and diameters, operating in other flow regimes need to be produced. It is also possible to implement other control strategies which are non-continuous such as latching.

Acknowledgment

The authors would like to acknowledge the support of Enterprise Ireland, who funded this work under grants TD/2006/0325 and TD/2009/0331.

References

[1] J. Falnes, "Optimum control of oscillation of wave-energy converters," in *Proceedings of the Eleventh (2001) International Offshore and Polar Engineering Conference,Stavanger, Norway, June 17-22.*, 2001.

[2] U. Korde, "Control system applications in wave energy conversion," in *Proceedings of the OCEANS 2000 MTS/IEEE Conference and Exhibition*, no. 3, 2000, pp. 1817–1724.

[3] ——, "Use of oscillation constraints in providing a reaction for deep water floating wave energy devices," *International Journal of Offshore and Polar Engineering*, vol. 11, no. 2, pp. 1473–1484, 2001.

[4] G. de Backer, M. Vantorre, C. Beels, J. de Rouck, and P. Frigaard, "Power absorption by closely spaced point absorbers in constrained conditions," *IET Renewable Power Generation*, vol. 4, no. 6, pp. 579–591, 2009.

[5] H. Eidsmoen, "Optimum control of a floating wave-energy converter with restricted amplitude," *Journal of Offshore Mechanics and Arctic Engineering*, vol. 118, no. 2, pp. 96–102, 1996.

[6] H. Eidsmoen, "Simulation of a slack-moored heaving-buoy wave-energy converter with phase control," Division of Physics, Norwegian University of Science and Technology NTNU, Trondheim, Norway, Technical report, 1996.

[7] J. Hals, J. Falnes, and M. Torgeir, "Constrained optimal control of a heaving buoy wave-energy converter," *Journal of Offshore Mechanics and Arctic Engineering*, vol. 133, p. 11401, 2011.

[8] F. Fusco and J. V. Ringwood, "Suboptimal and causal reactive control of wave energy converters through second order model reduction," in *Proceedings of the 21st International Offshore (Ocean) and Polar Engineering Conference, June 19-24*, Maui, Hawaii/USA, 2011.

[9] G. Bacelli, J. V. Ringwood, and J.-C. Gilloteaux, "A control system for a self-reacting point absorber wave energy converter subject to constraints," in *IFAC World Congress*, 2011.

[10] D. Evans, "Some theoretical aspects of three-dimensional wave-energy absorbers," in *Sympoisum on Ocean Wave Energy Utliziation, Gothenburg, Sweden.*, 1979.

[11] J. Falnes, "Radiation impedance matrix and optimum power absorbtion for interacting oscillators in surface waves," *Applied Ocean Research*, vol. 2, pp. 75–80, 1980.

[12] G. P. Thomas and D. Evans, "Arrays of three-dimensional wave-energy absorbers," *Journal of Fluid Mechanics*, vol. 108, pp. 67–88, 1981.

[13] P. McIver, "Some hydrodynamic aspects of arrays of wave energy devices," *Applied Ocean Research*, vol. 16, pp. 61–69, 1994.

[14] B. F. M. Child and V. Venugopal, "Non-optimal tuning of wave energy device arrays," in *2nd International conference on Ocean Energy (ICOE)*, 15-17 October, Brest, France, 2008.

[15] M. Folley and T. Whittaker, "The effect of sub-optimal control and the spectral wave climate on the performance of wave energy converter arrays," *Applied Ocean Research*, vol. 31, no. 4, pp. 260–266, 2009.

[16] J. Cruz, R. Sykes, P. Siddorn, and R. Eatock Taylor, "Estimating the loads and energy yield of arrays of wave energy converters under realistic seas," *IET Renewable Power Generation*, vol. 4, no. 6, pp. 488–497, 2010, hC.

[17] WAMIT Inc, *User Manual, Versions 6.4, 6.4 PC, 6.3, 6.3S-PC*, 2006.

[18] C.-H. Lee and J. N. Newman, "Computation of wave effects using the panel method," in *Numerical Models in Fluid-Structure Interaction*, ser. Advances in Fluid Mechanics, S. K. Chakrabarti, Ed. Southampton: WIT Press, 2005, vol. 18.

[19] J. Falnes, *Ocean waves and oscillating systems : linear interactions including wave-energy extraction*. Cambridge University Press, 2002.
[20] G. Bacelli and J. V. Ringwood, "A geometrical interpretation of force and position constraints in the optimal control of wave energy devices," in *9th European Wave and Tidal Energy Conference, EWTEC*, 2011.